Materials Science & Engineering A 580 (2013) 125–132

Contents lists available at SciVerse ScienceDirect

Materials Science & Engineering A

journal homepage: www.elsevier.com/locate/msea

Investigation of the effects of ultrasonic vibration-assisted micro-upsetting on brass

Jung-Chung Hung [a,*], Yu-Chung Tsai [b]

[a] Department of Mechanical Engineering, National Chin-Yi University of Technology, No. 57, Lane 215, Section 2, Zhongshan Road, Taiping District, Taichung County 411, Taiwan

[b] Department of Mechanical Engineering, National Chiao Tung University, 1001 Ta-Hsueh Road, HsinChu 30010, Tawan

ARTICLE INFO

Article history:
Received 20 February 2012
Received in revised form
21 February 2013
Accepted 19 April 2013
Available online 29 April 2013

Keywords:
Grain size
Micro-upsetting
Size-effect
Ultrasonic vibration

ABSTRACT

Ultrasonic vibration is widely applied in traditional metal forming to soften material and to increase formability. However, the effects of ultrasonic vibration on miniaturized workpieces must be studied before applying its benefits to metallic micro-forming.

This study investigates the effects of applying ultrasonic vibration to micro-forming, along with two other factors: specimen size and grain size. Conventional (without ultrasonic vibration) and ultrasonic vibration micro-upsetting experiments were conducted using brass (C2600). Specimens of three different dimensions ($\phi 3 \times 4.5$ mm, $\phi 2 \times 3$ mm, and $\phi 1 \times 1.5$ mm) and of three grain sizes (12 μm, 44 μm, and 90 μm) were used.

The conventional micro-upsetting (CMU) experiment revealed the size-effect in which flow stress decreased with the miniaturizing of the specimen. Flow stress also decreased as the grain size increased, but at a smaller magnitude than that of the size-effect. Results show that ultrasonic vibration-assisted micro-upsetting (UMU) decreased the flow stress effectively, especially in miniaturized specimens. The amount of decrease was related more to the dimension than to the grain size of the specimen.

© 2013 Elsevier B.V. All rights reserved.

1. Introduction

As modern technology continues to develop, manufacturers are producing increasingly more compact products on a massive scale to meet consumer's needs. Miniaturized critical components such as micro-locks, micro-screws, micro-bearings, micro-motors, micro-gears, and micro-pumps are used in many fields, including motor, biotech, aviation, and optoelectronics, to reduce material wasting, enhance spatial usage, and reduce energy consumption. To achieve high strength and good reliability for the long-term usage of the products, many plastic components are being replaced with metallic ones. These miniaturized metallic components are fabricated from micro-forming processes. Metallic micro-forming has the same features as traditional metal forming, such as flexibility in material selections, low material costs, low investment in equipment, high production rate, and ease of mass production.

Applying ultrasonic vibration in the forming process may be a feasible approach to achieve a higher formability of metallic micro-forming. Previous studies on ultrasonic vibration-assisted forming, such as drawing [1–6], bending [7,8], and extrusion [9], show that ultrasonic vibration can decrease flow stress (soften material) effectively, reduce friction, or reduce the forming limitations of traditional macro-scaled forming process. However, the effects of ultrasonic vibration on miniaturized workpieces must be studied before introducing its benefits into metallic micro-forming. Notable research on incorporating ultrasonic vibration in micro-scaled metallic forming has not yet been seen. Therefore, this study adopts micro-upsetting as a vehicle to investigate the effects of applying ultrasonic vibration to micro-scaled metallic forming.

The dimensions of miniaturized components lead to a rapid increase in their surface to volume ratio. As a result, forming mechanisms in metallic micro-forming are relatively different from those in the traditional macro-scaled forming process. The so-called "size-effect," in which the flow stress decreases with the miniaturizing of specimens during tension or upsetting, becomes a key factor in metallic micro-forming. The size-effect can be explained by the idea of the surface layer model (Fig. 1) introduced by Geiger et al. [10,11], Kals et al. [12], and Engel et al. [13,14]. The grains located at the surface of a tensile or upsetting specimen are less restricted than grains within the material. Dislocations moving through the grains during deformation pile up at grain boundaries, but not at the free surface. This leads to less hardening and lower deformation resistance in the surface grains. With decreasing specimen size and a size invariant microstructure, the share of

* Corresponding author. Tel.: +886 4 23924505 × 7192; fax: +886 4 23930681.
E-mail address: hjc@ncut.edu.tw (J.-C. Hung).

0921-5093/$ - see front matter © 2013 Elsevier B.V. All rights reserved.
http://dx.doi.org/10.1016/j.msea.2013.04.074

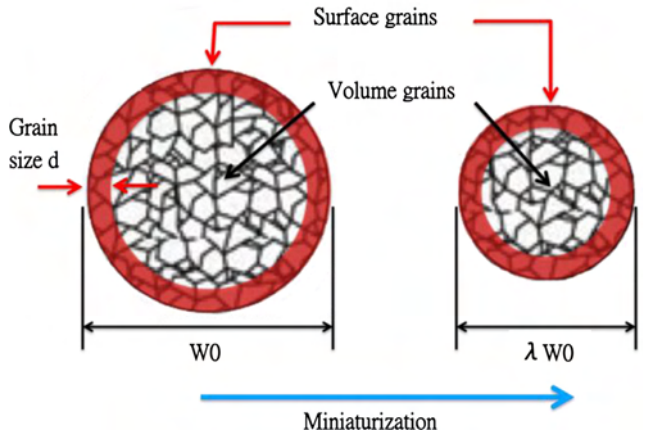

Fig. 1. Surface layer grain model. (W0: diameter of the specimen, λ: scaling factor).

surface grains increases, which leads to lower integral flow curves. The relationship between the grain size and the size-effect has been investigated in micro-upsetting (micro-compression) experiments (Chan et al. [15], Deng et al. [16] and Wang et al. [17]) and in micro-bending experiments (Nakamachi et al. [18], Raulea et al. [19], Gau et al. [20], and Shan et al. [21]). These studies were conducted with copper, aluminum, and brass, and all of their results demonstrate that the flow stresses decreased not only with miniaturized specimens, but also with enlarged grain sizes.

To investigate the effects of applying ultrasonic vibration along with the influence of the size-effect and grain size, this study presents both conventional and ultrasonic vibration assisted micro-upsetting experiments involving specimens with different dimensions and different grain sizes.

2. Experimental methods

2.1. Heat treatment for different grain sizes

Extruded brass rod was used in this research, and its grain size on the surface layer was significantly different from the inner grain size. Large residual stress inherited from extrusion remained in the specimen. Therefore, the specimens were heat treated to eliminate the residual stress and obtain different grain sizes for further investigation. Heat treatment was conducted under vacuumed condition to prevent oxidation of the brass. Specimens were placed into quartz tubes, and these tubes were vacuumed subsequently before they are sealed. These quartz tubes were then heated to 500 °C, 600 °C, and 700 °C and sustained for 2 h.

Specimens were etched using the recipe of ASTM E407-07, H_2O_2: 1 c.c. and NH_4OH: 49 c.c. for metallographic examinations. Fig. 2 shows the metallographic structures of the specimens with three different heat-treating temperatures (500 °C, 600 °C, and 700 °C). The grain sizes are 12 μm, 44 μm, and 90 μm, respectively.

2.2. Experimental procedures

Experiments were performed on a self-designed ultrasonic vibration micro-forming apparatus with 3 μm feeding and 0.5 N loading accuracies (Fig. 3). Table 1 lists the features of this apparatus. This apparatus used a down-sitting structure design, and all motors were mounted at the bottom of the apparatus to increase stability and to prevent elevated temperatures damaging the sensor units during processing. This apparatus includes a self-designed booster and resonator along with a 2 kW generator (King Ultrasonic Co., KWS2020). A vibrating frequency of 20 kHz with an amplitude of 2.5 μm was applied on the axial direction in the experiments.

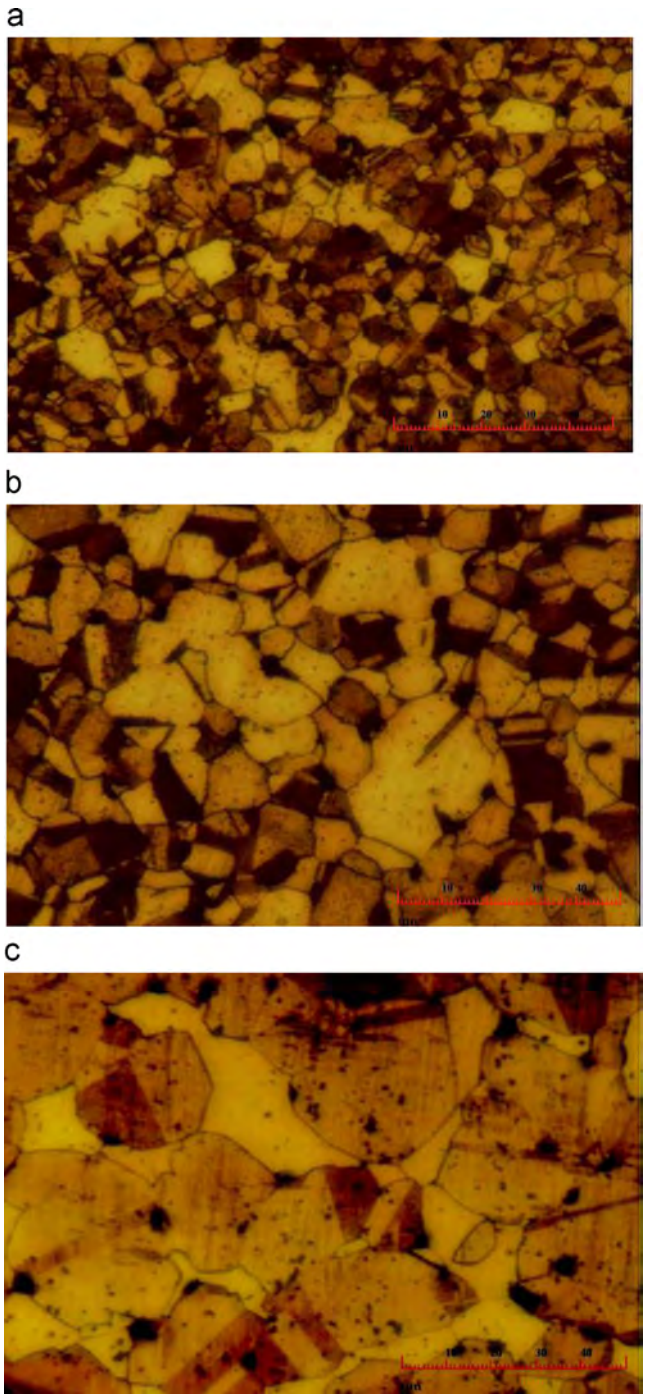

Fig. 2. Metallographic structures of specimens under three different heat-treating temperatures (500 °C, 600 °C and 700 °C). (a) 500°C (grain size: 12 μm), (b) 600 °C (grain size: 44 μm) and (c) 700°C (grain size: 90 μm).

Alloy tool steel was used as the mold material and blue moly was used as a lubricant to reduce interfacial friction between molds and specimens. A specimen measuring 3 mm in diameter (ϕ) and 4.5 mm in height served as a dimensional standard. A scaling factor λ was introduced to represent the geometric similarity in diameter of the miniaturized specimens: $\lambda=1$ represents a specimen of $\phi 3.0 \times 4.5$ mm. Two other scaling factors, $\lambda=0.67$ and $\lambda=0.33$, were used to represent the specimens of $\phi 2.0 \times 3$ mm and $\phi 1.0 \times 1.5$ mm, respectively. In the ultrasonic vibration-assisted micro-upsetting experiments, ultrasonic vibration was applied when the compressive

force reached 500 N, 300 N, and 150 N, respectively, for specimens with scaling factors of $\lambda=1$, 0.67, and 0.33. Conventional and ultrasonic vibration assisted micro-upsetting experiments were performed with three different sizes of specimens with three kinds of grain sizes. Table 2 presents the experimental conditions.

3. Conventional micro-upsetting (CMU) experiment

3.1. Size-effect

Figs. 4–6 show the CMU stress–strain (σ–ε) relationships of specimens with three different sizes (scaling factors of $\lambda=1$, 0.67, and 0.33) under the condition of the same grain sizes (12 μm, 44 μm, and 90 μm). The maximum flow stress of different scaling factors with various grain sizes and the decrease of maximum flow stress compared to the specimen with $\lambda=1$ are shown in Tables 3–5. Lower flow stress was exhibited by the specimens with a smaller scaling factor (Consider the results of 90 μm grains for example, when $\lambda=0.33$, the maximum stress is 573 MPa; when $\lambda=0.67$, the maximum stress is 615 MPa; and when $\lambda=1$, the maximum stress is 640 MPa.). The surface layer model [10–14] may be used to explain this phenomenon (Fig. 1). For microparts, the share of grains representing the surface layer becomes high compared to the grains

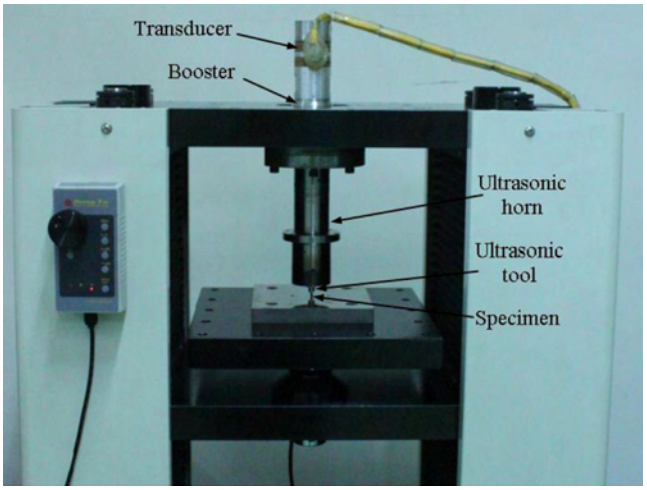

Fig. 3. Ultrasonic vibration micro-forming apparatus.

Table 1
Features of self-designed micro-forming apparatus.

Maximum loading	10,000 N
Drivers	Servo motor
Feeding speed	0.5–200 mm/min
Feeding accuracy	3 μm
Control type	Close-loop

Table 2
Material and micro-upsetting conditions.

Specimen material	Brass (C2600)
Tooling material	Alloy tool steel (SKD11)
Scaling factors (λ)	1, 0.67, and 0.33
Size of specimen	$\phi3.0\times4.5$ mm, $\phi2.0\times3$ mm, and $\phi1.0\times1.5$ mm
Size of grain	12 μm, 44 μm, and 90 μm
Punch speed	1 mm/min, 0.6 mm/min, and 0.3 mm/min
Reduction (R)	50%
Lubricant	Blue moly

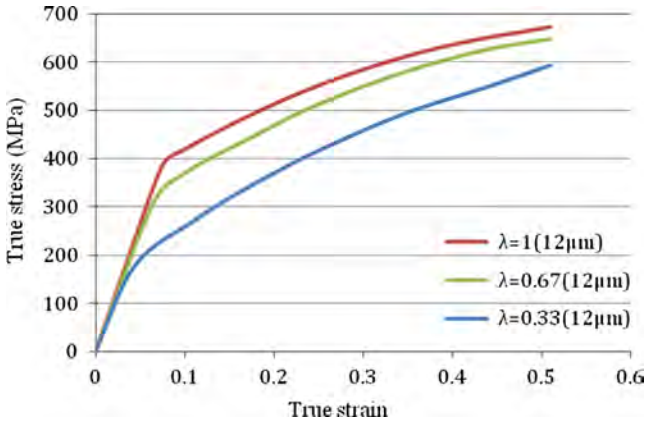

Fig. 4. CMU stress–strain relationships of specimens with three different scaling factors (grain size of 12 μm).

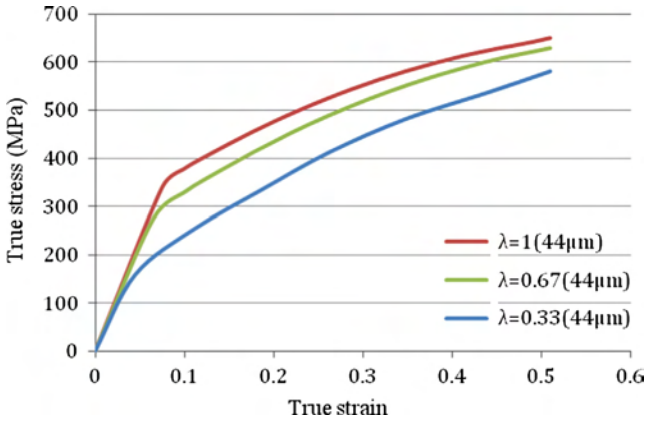

Fig. 5. CMU stress–strain relationships of specimens with three different scaling factors (grain size of 44 μm).

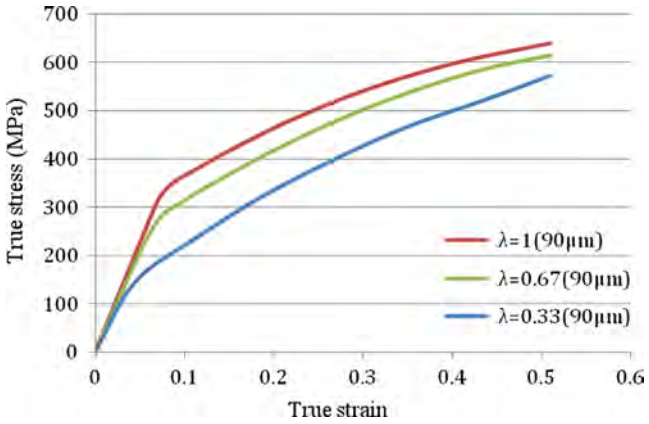

Fig. 6. CMU stress–strain relationships of specimens with three different scaling factors (grain size of 90 μm).

Table 3
Maximum flow stress with different scaling factors and the decrease of maximum flow stress compared to the specimen with $\lambda=1$ (grain size: 12 μm).

Scaling factor (λ)	Max. (at $\varepsilon=0.7$) (MPa)	Max. stress decrease (compared to max. stress of $\lambda=1$) (MPa)
1	673	–
0.67	649	24
0.33	594	79

that are surrounded entirely by other grains. From metal physics theory it is known that free surface grains show less hardening compared to the inner volume grains which can be explained by the different mechanisms of dislocation movement and pile up and by the fact that they are less subjected to compatibility restrictions [13].

Table 4
Maximum flow stress with different scaling factors and the decrease of maximum flow stress compared to the specimen with $\lambda=1$ (grain size: 44 μm).

Scaling factor (λ)	Max. (at $\varepsilon=0.7$) (MPa)	Max. stress decrease (compared to max. stress of $\lambda=1$) (MPa)
1	651	–
0.67	625	26
0.33	582	69

Table 5
Maximum flow stress with different scaling factors and the decrease of maximum flow stress compared to the specimen with $\lambda=1$ (grain size: 90 μm).

Scaling factor (λ)	Max. (at $\varepsilon=0.7$) (MPa)	Max. stress decrease (compared to max. stress of $\lambda=1$) (MPa)
1	640	–
0.67	615	25
0.33	573	67

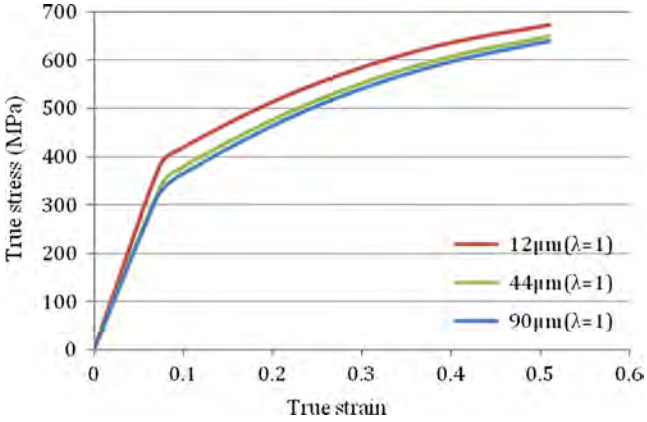

Fig. 7. CMU stress–strain relationships of specimens with three different grain sizes (scaling factor $\lambda=1$).

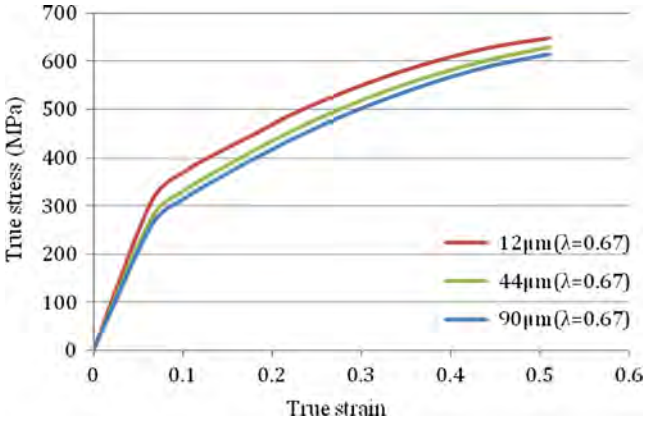

Fig. 8. CMU stress–strain relationships of specimens with three different grain sizes (scaling factor $\lambda=0.67$).

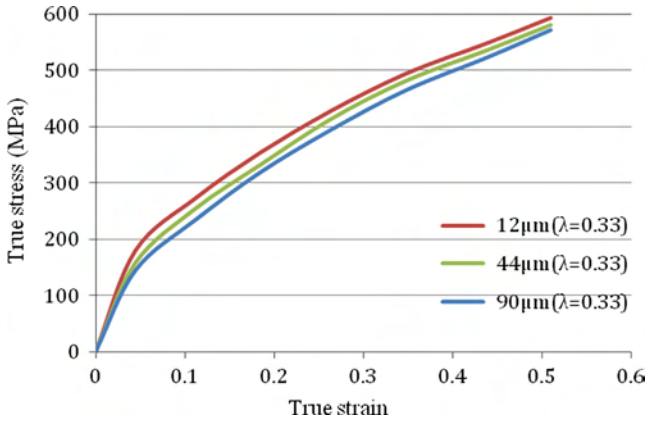

Fig. 9. CMU stress–strain relationships of specimens with three different grain sizes (scaling factor $\lambda=0.33$).

Table 6
Flow stress reduction of different scaling factors when comparing maximum (90 μm) to minimum (12 μm) grain sizes.

Scaling factor (λ)	Flow stress reduction (MPa) (|(grain size 90 μm)–(grain size 12 μm)|)
1	33
0.67	34
0.33	22

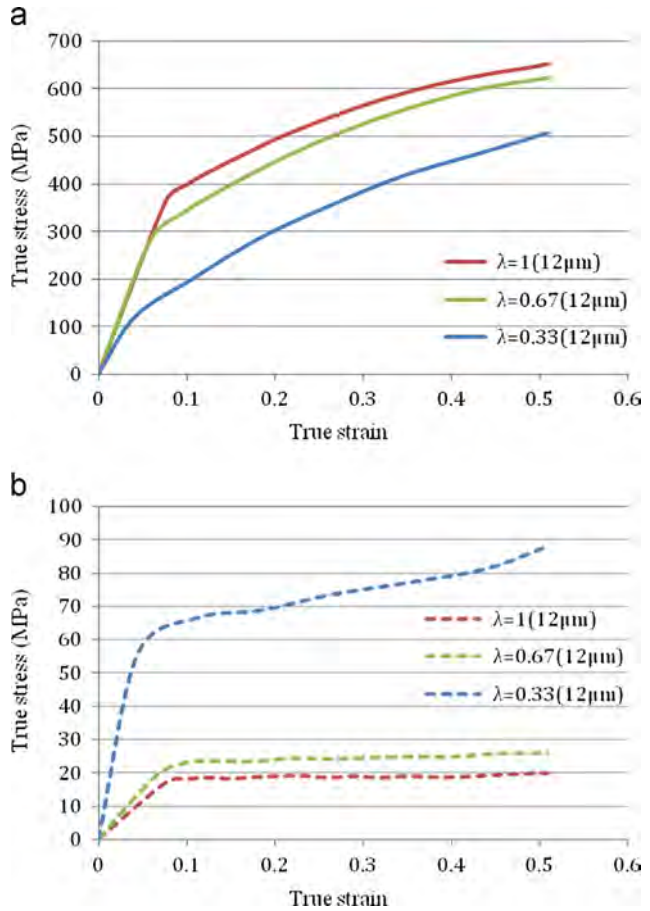

Fig. 10. UMU stress–strain relationships of specimens with three different scaling factors (grain size of 12 μm). (a) UMU results with three different scaling factors. (b) Comparing UMU to CMU results (CMU–UMU).

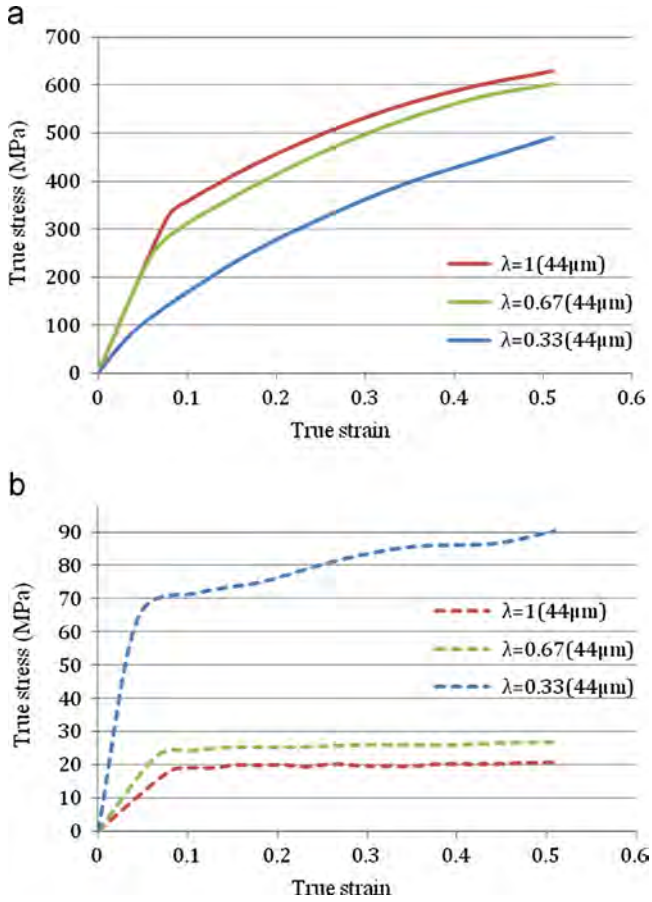

Fig. 11. UMU stress–strain relationships of specimens with three different scaling factors (grain size of 44 μm). (a) UMU results with three different scaling factors. (b) Comparing UMU to CMU results (CMU–UMU).

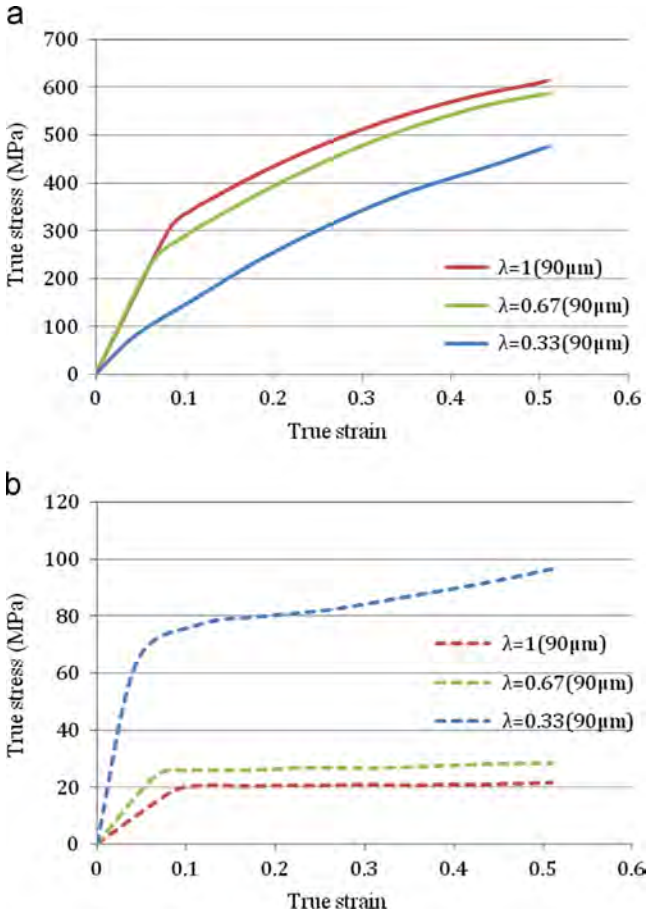

Fig. 12. UMU stress–strain relationships of specimens with three different scaling factors (grain size of 90 μm). (a) UMU results with three different scaling factors. (b) Comparing UMU to CMU results (CMU–UMU).

3.2. *Effects of grain size*

Figs. 7–9 show the CMU stress–strain (σ–ε) relationships of specimens with λ=0.33, 0.67, and 1. Table 6 shows the flow stress reduction of different scaling factors by comparing the results for the maximal (90 μm) to minimal (12 μm) grain sizes. The decrease in flow stress resulting from an increase of grain size (the increase of heat treating temperature) is not as obvious as the size-effect, especially for smaller specimens (λ=0.33). This may be because the ratio of grain size to volume increases when specimens were miniaturized, and the constraints of grain boundaries, regardless of whether volume grains or surface grains, decrease. Thus, the flow stresses of specimens with different grain sizes under the same scaling factor revealed little deviation.

4. Effects of applying ultrasonic vibration

4.1. *Ultrasonic vibration with different specimen sizes*

The results of ultrasonic vibration-assisted micro-upsetting (UMU) demonstrated a trend similar to those of CMU in that the flow stresses decreased with the miniaturizing of specimens (Figs. 10a, 11a, and 12a). After comparing to the CMU results (CMU–UMU), the flow stress clearly decreased by applying ultrasonic vibration (Figs. 10b, 11b, and 12b) A smaller specimen indicated a greater decrease. The amount of flow stress reduced by the three scaling factors for various grain sizes is shown in Tables 7–9. The results for the three grain sizes show that the

Table 7
The amounts of decreased flow stress with different scaling factors (grain size: 12 μm).

Scaling factor (λ)	Avg. (from ε=0.1 to 0.7) (MPa)	Max. (at ε=0.7) (MPa)
1	18.79	19.91
0.67	23.89	25.83
0.33	73.12	88.24

Table 8
The amounts of decreased flow stress with different scaling factors (grain size: 44 μm).

Scaling factor (λ)	Avg. (from ε=0.1 to 0.7) (MPa)	Max. (at ε=0.7) (MPa)
1	19.78	20.75
0.67	25.37	26.76
0.33	79.30	90.36

Table 9
The amounts of decreased flow stress with different scaling factors (grain size: 90 μm).

Scaling factor (λ)	Avg. (from ε=0.1 to 0.7) (MPa)	Max. (at ε=0.7) (MPa)
1	20.59	21.58
0.67	26.61	28.40
0.33	82.53	96.49

specimen with $\lambda=0.33$ exhibited the greatest decrease compared to the specimens with $\lambda=0.67$ and $\lambda=1$ (Consider the results of the 90 μm grains for example, when $\lambda=0.33$, the average reduction of stress was 82.53 MPa and the maximum reduction was 96.49 MPa; when $\lambda=0.67$, the average reduction of stress was 26.61 MPa, and maximum reduction was 28.40 MPa; and when $\lambda=1$, the average reduction of stress was 20.59 MPa and the maximum reduction was 21.58 MPa.). The possible mechanisms of these significant reductions resulting from ultrasonic vibration are discussed in Section 4.3.

4.2. Ultrasonic vibration with different grain sizes

Figs. 13–15 show the stress–strain (σ–ε) relationships of ultrasonic vibration-assisted micro-upsetting (UMU) for specimens with $\lambda=1$, 0.67, and 0.33. These results demonstrate that the decrease in flow stress along with the increase of grain size is not as significant as the effects on the UMU with different specimen sizes (Figs. 13b, 14b, and 15b). That is, the decrease in flow stress for specimens with smaller grain sizes under the same scaling factor exhibited little deviation. Explanations on these experimental results are addressed in Section 4.3 as well.

4.3. Discussion on the effects of applying ultrasonic vibrations in micro-upsetting on brass

Many research works suggested that ultrasonic energy is absorbed in the highly localized regions such as dislocations, voids and grain boundaries. The ultrasonic energy causes the speed of dislocations to increase such that the extended ones contract into unit dislocations, which then cross glide freely without the aid of thermal activation [22–24]. Fig. 16a and b shows the metallographic structure of a CMU, and Figs. 17a and b shows the metallographic structure of UMU. Fig. 17a and b shows that the deformations in the shear band area in UMU are larger than of those in CMU (Fig. 16a and b). This may indicate that the ultrasonic energy was absorbed in this localized area and the speed of dislocations is increased during deformation thus result in lower flow stress and larger plastic deformation in UMU.

In Section 4.1, with the same amount of applied vibrating amplitude and frequency, the absorbed energy per volume increases while the scale of specimen decreases. Hence, when specimens are scaled down to $\lambda=0.33$, significant flow stress reduction appears. As to Section 4.2, for the specimens with the same scaling factors but different grain sizes, since the ultrasonic energy is absorbed in highly localized regions, the obstacles need to overcome mainly locate in the shear band area and the amount of these obstacles may not differ much for these specimens. Therefore variation in grain sizes exhibited little influence on the deviation of flow stress.

Furthermore, to investigate whether thermal softening plays a significant role in the reduction of flow stress, we performed temperature measurements in UMU with three scaling factors using flange-shaped specimens with K-type thermocouples (thermocouple diameter: 0.17 mm) (Fig. 18) to monitor the temperature variations of the mold-specimen interface, that is, the ultrasonic vibration interface. The monitored results (Fig. 19) showed that the

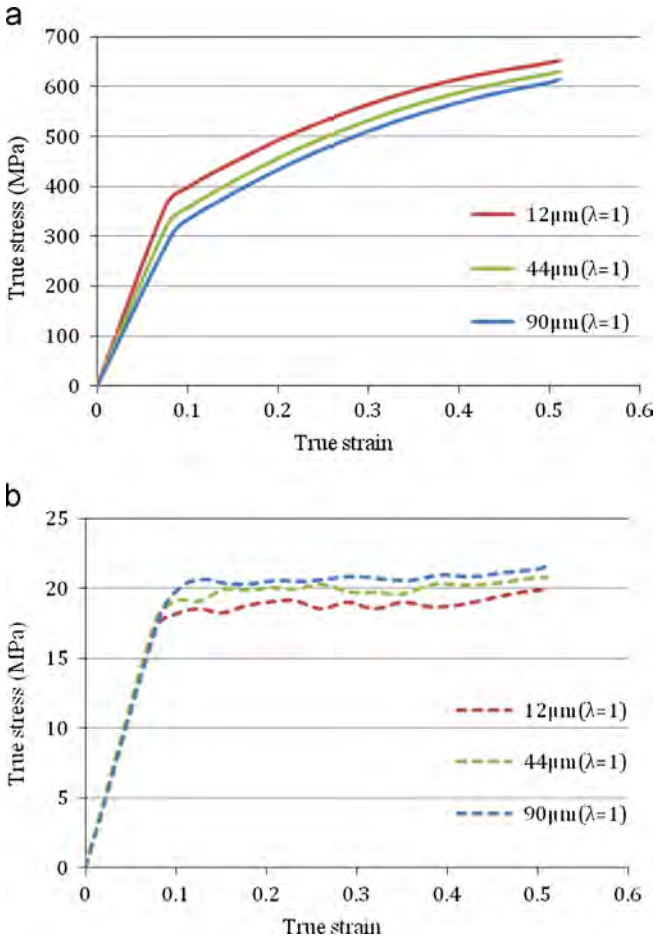

Fig. 13. UMU stress–strain relationships of specimens with three different grain sizes (scaling factor $\lambda=1$). (a) UMU results with three different grain sizes. (b) Comparing UMU to CMU results (CMU–UMU).

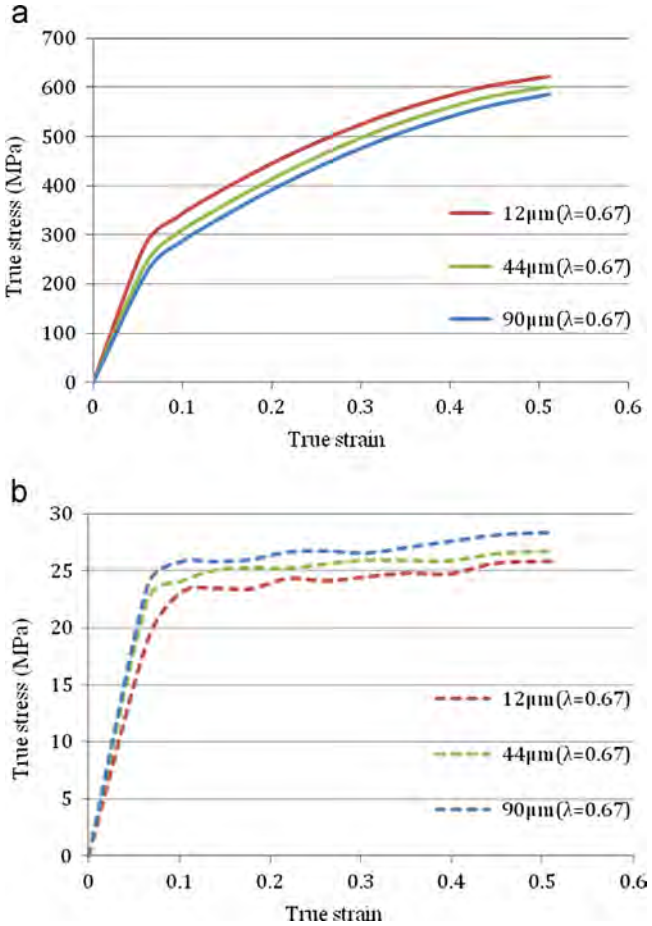

Fig. 14. UMU stress–strain relationships of specimens with three different grain sizes (scaling factor $\lambda=0.67$). (a) UMU results with three different grain sizes. (b) Comparing UMU to CMU results (CMU–UMU).

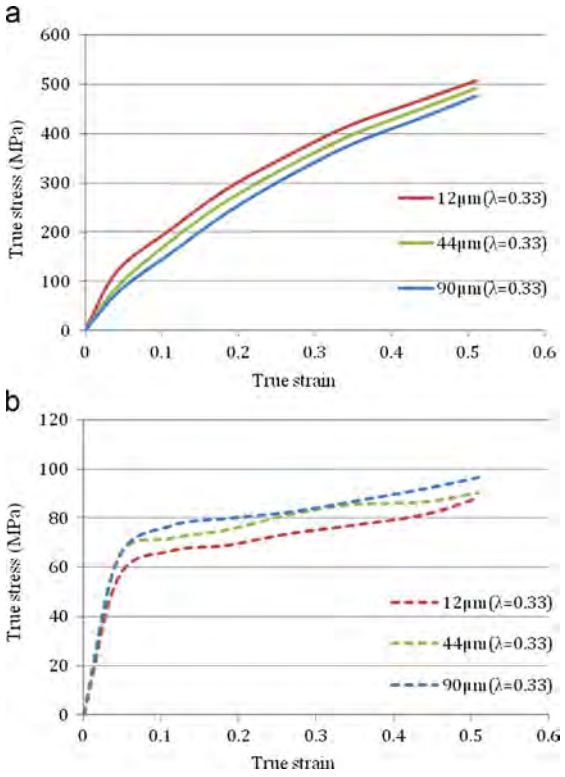

Fig. 15. UMU stress–strain relationships of specimens with three different grain sizes (scaling factor $\lambda=0.33$). (a) UMU results with three different grain sizes. (b) Comparing UMU to CMU results (CMU–UMU).

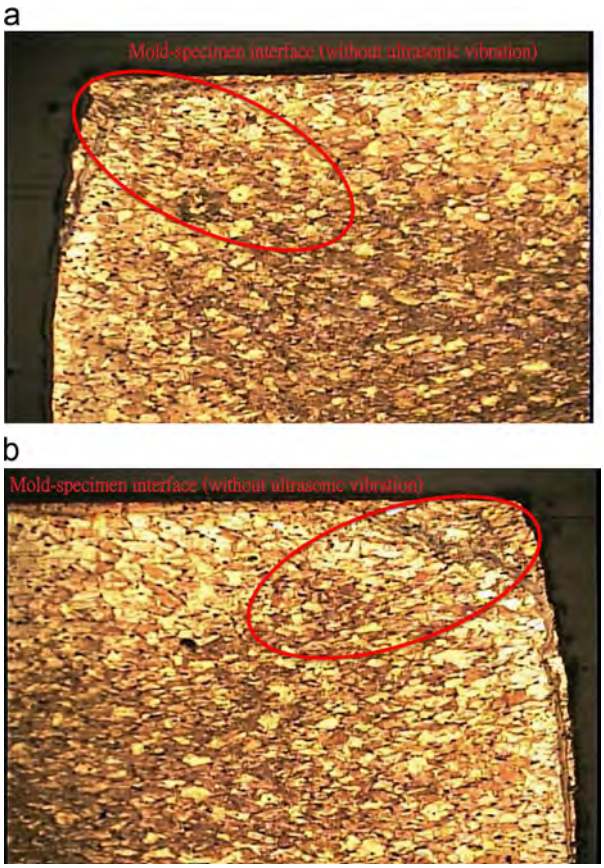

Fig. 16. Metallographic structure of CMU ($\lambda=0.67$, grain size$=90$ μm) (a) deformation of grains near the mold-specimen interface (without ultrasonic vibration) (upper left) and (b) deformation of grains near the mold-specimen interface (without ultrasonic vibration) (upper right).

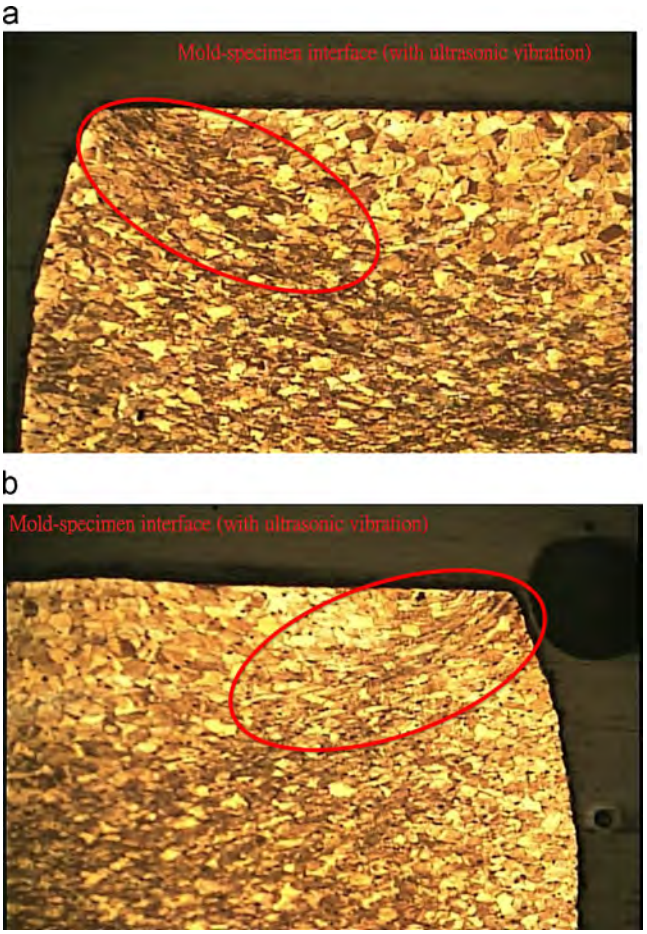

Fig. 17. Metallographic structure of UMU ($\lambda=0.67$, grain size$=90$ μm) (a) deformation of grains near the mold–specimen interface (with ultrasonic vibration) (upper left) and (b) deformation of grains near the mold–specimen interface (with ultrasonic vibration) (upper right).

temperatures did not increase significantly when ultrasonic vibration was applied. Even in the smallest specimen ($\lambda=0.33$), the temperature only increased by 3.5 °C. However, to achieve this level of stress reduction, temperatures should be increased to over 100 °C. In other words, the results of this study showed that thermal softening has insignificant influence on the stress reduction phenomenon.

5. Conclusion

This study uses conventional micro-upsetting (CMU) and ultrasonic vibration-assisted micro-upsetting (UMU) experiments to investigate the effects of size-effect, grain size, and ultrasonic vibration. The conclusions of this study are as follows:

1. The CMU experimental results demonstrate the size effect, where the flow stress decreases as the specimen is miniaturized. But the flow stress decrease was relatively minimal while increasing the grain size of the specimens with the same scaling factors in CMU.
2. The UMU experimental results show that applying ultrasonic vibration in micro-upsetting effectively reduced flow stress. This may because the ultrasonic energy is absorbed in the highly localized regions and causes the speed of dislocations to increase thus result in larger deformations in the shear band area in UMU as demonstrated in this study.

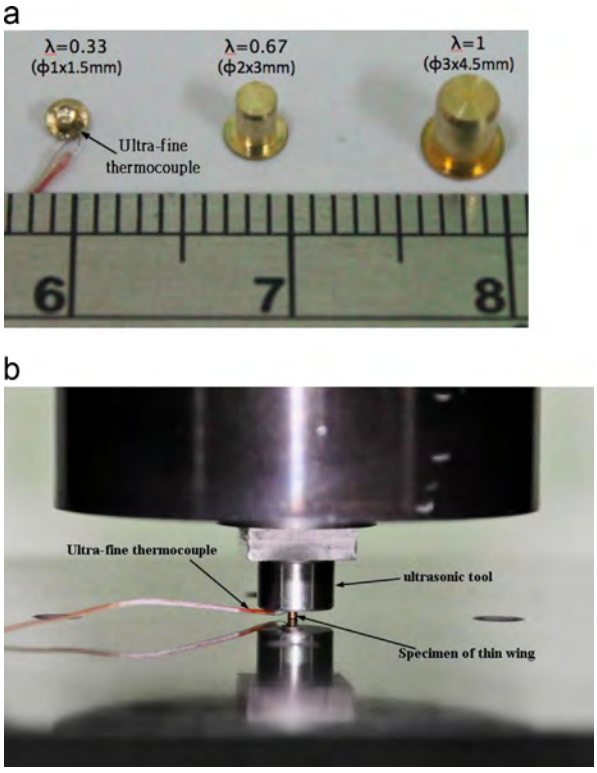

Fig. 18. Flange-shaped specimens for three scaling factors with K-type thermocouples (thermocouple diameter: 0.17 mm) (a) flange-shaped specimens for three scaling factors and (b) installation of temperature measurement experiments.

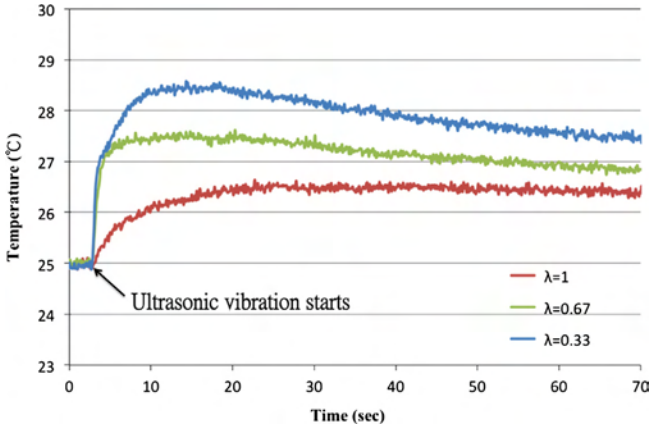

Fig. 19. Temperatures increases under ultrasonic vibrations.

3. The decrease in flow stress for specimens with smaller grain sizes under the same scaling factor exhibited minimal deviation.
4. Thermal softening when applying ultrasonic vibrations was insignificant in this study.
5. For this study, we emphasized the effects of ultrasonic vibration-assisted micro-upsetting on brass using three scale specimens ($\phi 3 \times 4.5$ mm, $\phi 2 \times 3$ mm, and $\phi 1 \times 1.5$ mm). Investigations can be extended to larger-scale specimens (e.g., $\phi 4 \times 6$ mm) and smaller-scale specimens (e.g., $\phi 0.8 \times 1.2$ mm) to explore the trends of stress reduction more extensively in the future.

Acknowledgment

The authors would like to thank the National Science Council of Taiwan, ROC for the grant NSC98-2221-E-167 -005, under which the investigation was undertaken.

References

[1] J.T. Buckley, M.K. Freeman, Ultrasonics 8 (1970) 152–158.
[2] K. Siegert, J. Mater. Process. Tech. 60 (1996) 657–660.
[3] T. Jimma, J. Mater. Process. Tech. 80-81 (1998) 406–412.
[4] M. Murakawa, P. Kaewtatip, M. Jin, Trans. NAMRI/SME 28 (2000) 75–80.
[5] M. Murakawa, M. Jin, J. Mater. Process. Tech. 113 (2001) 81–86.
[6] M. Hayashi, J. JSTP 42 (2001) 1070–1074.
[7] J. Tsujion, Proceedings of IEEE 1989 Ultrasonic Symposium 1099–1102.
[8] J. Tusjion, Proceedings of IEEE 1992 Ultrasonic Symposium 1863–866.
[9] M. Jin, Adv. Tech, Plasticity 3 (1999) 19–24.
[10] M. Geiger, M. Kleiner, R. Eckstein, N. Tiesler, U. Engel, Ann. CIRP 50 (2001) 445–462.
[11] M. Geiger, A. Mebner, U. Engel, Prod. Eng. 4 (1) (1997) 55–58.
[12] T.A. Kals, R. Eckstein, J. Mater. Process. Tech. 103 (2000) 95–101.
[13] U. Engel, R. Eckstein, J. Mater. Process. Tech. 125–126 (2002) 35–44.
[14] U. Engel, R. Eckstein, J. Mater. Process. Tech. 125–126 (2002) 95–101.
[15] W.L. Chan, M.W. Fu, J. Lu, J.G. Liu, Mat. Sci. Eng. A 527 (2010) 6638–6648.
[16] J.H. Deng, M.W. Fu, W.L. Chan, Mat. Sci. Eng. A 528 (2011) 4799–4806.
[17] C.J. Wang, B. Guo, D.B. Shan, L.N. Sun, T. Nonferr. Metal. Soc. 19 (2009) 511–515.
[18] E. Nakamachi, K. Hiraiwa, H. Morimoto, M. Harimoto, Int. J. Plasticity 16 (2000) 1419–1441.
[19] L. V. Raulea, A. M. Goijaerts, L. E. Govaert, F. P. T. Baaijens, J. Mater. Process. Tech. 115 (2001) 44-48.
[20] J.T. Gau, C. Principe, J. Wang, J. Mater. Process. Tech. 184 (2007) 42–46.
[21] D.B. Shan, C.J. Wang, B. Guo, X.W. Wang, T. Nonferr. Metal. Soc. 19 (2009) 507–510.
[22] A. Siddiq, T.E. Sayed, Mater. Lett. 65 (2011) 356–359.
[23] J.J. Gilman, Mat. Sci. Eng. A 319–321 (2001) 84–86.
[24] Z. Yao, G.Y. Kim, L. Faidley, Q. Zou, D. Mei, Z. Chen, J. Manuf. Sci. Eng. 133 (2011) 061009-1–8.